Surface Science 186 (1987) 393–411
North-Holland, Amsterdam

A MODEL STUDY OF ALKALI PROMOTION OF WATER–GAS SHIFT CATALYSTS: Cs/Cu(111)

Charles T. CAMPBELL *

Chemistry Department, Indiana University, Bloomington, IN 47405, USA **

and

Bruce E. KOEL

Cooperative Institute for Research in Environmental Sciences, and Chemistry Department, University of Colorado, Boulder, CO 80305, USA

Received 4 December 1986; accepted for publication 12 March 1987

The kinetics of the forward water–gas shift reaction ($H_2O + CO \rightarrow H_2 + CO_2$) have been measured on a Cs-doped Cu(111) single-crystal surface at pressures near 40 Torr. The Cs is dosed from aqueous CsOH solution and dried in air. The surface structures have been characterized by XPS, AES, LEED, and ISS both before and after reaction. The activity of the Cu(111) surface increases with increasing Cs coverage until it reaches a maximum at $\theta_{Cs} \approx 0.13$, where the rate is fifteen times that for Cs-free Cu(111). At higher coverages the rate decreases. The as-dosed surface is oxidized to Cu_2O to a depth ≥ 20 Å. After brief treatments (< 40 s) under reaction conditions, the surface is completely reduced to metallic Cu(111), with a Cs overlayer showing an O:Cs atomic ratio of about unity. This overlayer demonstrates a $p(2\times2)$ LEED pattern when θ_{Cs} exceeds 0.13 (where the rate maximizes), which is interpreted in terms of islands of an oxidic or hydroxidic Cs overlayer of local coverage $\theta_{Cs} = 1/4$. The promotion by Cs is attributed to a mechanism where the surface Cs/O complex participates directly in the dissociation of adsorbed H_2O, which is the rate-determining step.

1. Introduction

The solid-catalyzed, forward water–gas shift reaction ($H_2O + CO \rightarrow H_2 + CO_2$) is a step in numerous industrial processes including hydrogen production and ammonia synthesis. Proposed technologies for utilizing our fossil fuel resources, such as coal gasification, depend on the use of water–gas shift catalysts to upgrade hydrogen content. Catalysts based on Cu/ZnO mixtures have received broad industrial acceptance in water–gas shift (WGS), since their high activities permit low temperature operation and consequently higher thermodynamic conversion limits [1]. These unfortunately poison readily at

* Alfred P. Sloan Research Fellow.
** Experiments performed at Los Alamos National Laboratory.

very low sulfur levels, and are therefore not ideal for fossil-fuel-based feedstreams [1]. Thus, there is considerable practical incentive for developing a fundamental understanding of this reaction and the relationships among catalyst activity, sulfur tolerance, and surface structure. Nevertheless, relatively little work has been published in this area ([1–11] and references therein).

In a recent study [10], we have shown that the Cu(111) single-crystal surface is a good kinetic model of high-surface-area Cu/ZnO catalysts for this reaction, and that metallic Cu seems to provide the active sites. Furthermore, we have modeled the sulfur poisoning of this reaction on Cu(111) using adsorbed sulfur adatoms deposited from H_2S gas [11]. These studies indicated that the dissociative adsorption of water was the rate-determining step under our reaction conditions. Since alkali metals are thought to promote water dissociation on other transition metal surfaces such as Ru [12,13] and Pt [14], we have attempted to promote the Cu(111) model catalyst using alkali overlayers. The results presented here show that, with proper Cs addition, an enhancement in the WGS activity by a factor of ~ 15 can result. This is consistent with very recent reports by Klier et al. [7,8] that Cs doping can lead to a two-fold enhancement in the WGS activity of high-area Cu/ZnO catalysts at lower temperature and higher pressure conditions.

In addition to demonstrating the Cs promotion of Cu(111) for WGS, we study here the structure of the surface after dosing with Cs (from aqueous CsOH solution) and after treatment under reaction conditions. We also investigate the potential of Cs additives for improving the tolerance of Cu(111) in sulfur poisoning.

2. Experimental

The apparatus and procedures for studying the WGS reaction on clean Cu(111) [10] and for dosing H_2S [11] have been described in detail previously. The sample surface was cleaned and analyzed in ultrahigh vacuum (UHV), then translated outside the vacuum chamber and dosed with a droplet of aqueous CsOH solution, heated to ~ 390 K for 30 s to dry the droplet, then translated back into UHV. We have described this type of Cs dosing for Ag(111) previously, and shown that it produces the same final Cs surface structure as that resulting from the vapor-deposition of Cs followed by use as an ethylene oxidation catalyst [15]. After characterizing the as-dosed Cs overlayer by surface analyses (AES, XPS, ISS, LEED), the sample was translated into the batch microreactor, pressurized with the reaction mixture, then heated to the reaction temperature for the desired time. Product buildup was monitored with gas chromatography (GC). At the end of the desired reaction time, the sample was rapidly (~ 6 s) quenched to 465 K in the reaction mixture, then translated back into UHV for surface analysis.

Coverages (θ) are reported here in absolute units (per Cu surface atom), so that $\theta = 1$ corresponds to 1.76×10^{15} cm^{-2}.

The CsOH solutions were prepared from aqueous, research-grade CsOH solutions, diluted with ultrapure (HPLC grade) water. Well-conditioned polyethylene labware [16] was used in all steps of the dilution and dosing, to prevent contamination by impurities leached from container walls. Analyses by AES showed Cs and O to be the only elements added in measureable quantity to the surface upon Cs dosing. (Hydrogen is not detected in AES.)

The Cu(2p), valence band and Cs(3d) XPS and Cu(LVV) XAES spectra were recorded with Mg(Kα) radiation at a pass energy of 50 eV, which gave a Cu($2p_{3/2}$) peak for clean Cu(111) with a 1.3 eV FWHM (full-width at half-maximum). The O(1s) and S(2p) spectra were recorded with Al(Kα) radiation at a pass energy of 100 eV, which gave a Cu($2p_{3/2}$) for clean Cu(111) of 1.8 eV FWHM. (These Cu FWHMs can be taken as the overall instrumental resolutions.) Spectra are referenced to the Fermi level, so the Cu($2p_{3/2}$) peak is centered at 932.4 eV BE (binding energy). Detection was normal to the surface in AES, XPS, XAES and ISS. The ISS spectra were recorded with a 970 eV He^+ incident beam at 60° from the surface normal, using a pass energy of 1/3 the kinetic energy. The AES spectra were recorded with a 2900 eV electron beam, incident 60° from the surface normal, using a pass energy of 1/3 the kinetic energy and a modulation voltage of 5 $V_{p\text{-}p}$.

3. Results

3.1. Cs / Cu(111)

3.1.1. Influence on reaction kinetics

A typical plot of product (CO_2 and H_2) buildup versus WGS reaction time at 612 K, 26 Torr CO and 10 Torr H_2O is shown in fig. 1 for clean Cu(111) (from ref. [10]), and for Cs-dosed Cu(111). The reaction rate (slope) is much higher for the Cs-dosed surface at all reaction times. For both surfaces, the rate decreases significantly during the first four minutes, but the shape of the curve is about the same for both. For this reason, we feel justified in using product buildup over a fixed reaction time interval in comparing reaction rates for different Cs coverages. Note that, for the Cs-dosed surface, a total of ~ 1300 molecules of H_2 and of CO_2 are produced *per Cu surface atom* in a period of 19 min. At this point, the H_2O conversion would be rather high (~ 14%), except that, for the Cs-dosed surface, we used a fresh reaction mixture after every data point of fig. 1. In this way, we kept the conversion low (< 6%) to prevent back reaction of products. Thus, the product buildup data are added from successive measurements with the same surface (no cleaning between runs). The decrease in reaction rate with reaction time is

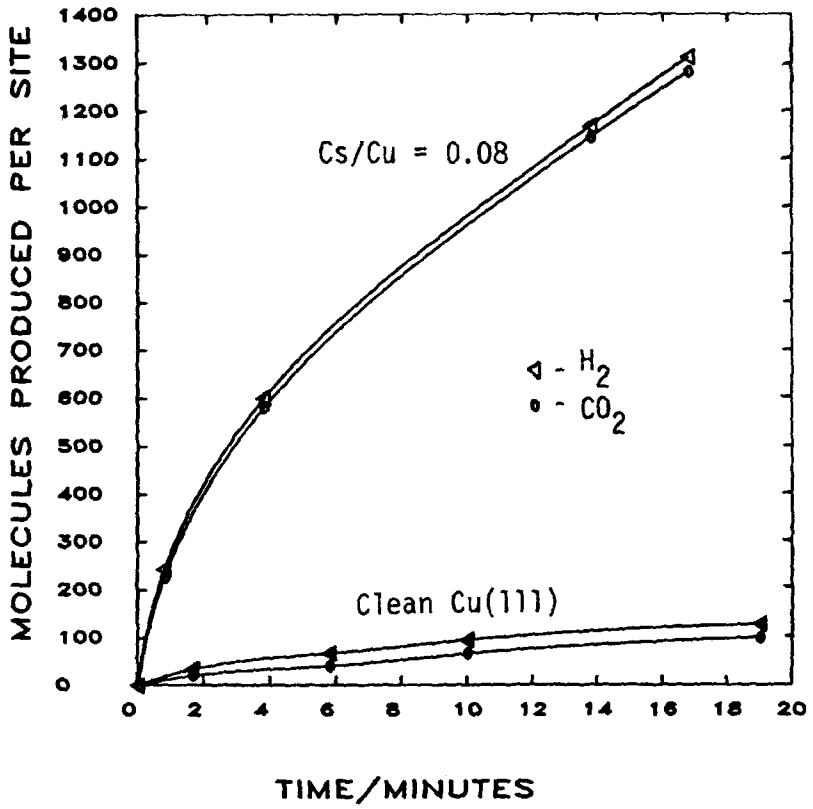

Fig. 1. Product buildup versus reaction time at 612 K in 26 Torr CO and 10 Torr H_2O for clean Cu(111) (solid points) and for the same surface after dosing with Cs (open points) to a level which gave a final Cs/Cu AES ratio of 0.08. Clean surface data from ref. [10].

therefore not due to an increased contribution from the reverse reaction, and must be related to a real change in the surface structure.

As will be described below, the surface structure and Cs concentration changed considerably in the first ~ 40 s of reaction time, after which it was almost constant. For this reason, we always reduced the as-dosed surface for 40 s in the reaction mixture and returned the sample to UHV for surface analysis before attempting kinetic measurements. In this way the Cs coverage and structure were almost constant during the rate measurement. We used the final coverage measured after reaction in reporting Cs coverages here. For the reduced surfaces, we have assumed the Cs(565 eV)/Cu(920 eV) AES peak-to-peak ratio to be proportional to θ_{Cs} here. We will refer to this ratio simply as "Cs/Cu" below. The data of fig. 1 are for Cs/Cu = 0.08.

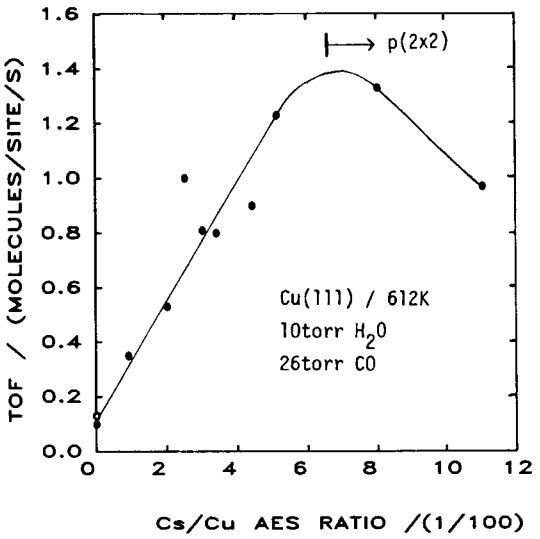

Fig. 2. Variation of the water–gas shift reaction rate with cesium coverage on Cu(111) at 612 K, 26 Torr CO and 10 Torr H_2O. The open data point was for dosing pure water (no CsOH). The data here represent the average rate between 0.67 and 4.67 min reaction time.

Fig. 2 shows the variation in WGS reaction rate with Cs coverage (Cs/Cu) at 612 K, 26 Torr CO and 10 Torr H_2O. (The absolute coverage calibration will be described below.) This rate shown here is the average rate between 0.67 and 4.67 min reaction time. As seen in fig. 1, this corresponds to a maximum H_2O conversion of ~ 7%. Therefore, we are essentially in the limit of low conversion here. In this paper we have studied the kinetics at temperatures (564–658 K) that are somewhat higher than typically used for Cu/ZnO catalysts (475–550 K). This is because, on the very low-surface-area single crystal, it is difficult to achieve measureable rates at much lower temperatures. As can be seen in fig. 2, the rate increases rapidly with θ_{Cs}, reaches a maximum at Cs/Cu = 0.075 ($\theta_{Cs} \simeq 0.13$), and then decreases somewhat. Higher coverages than those shown here were not stable under the reaction conditions at 612 K and could not be studied. The maximum rate is a factor of about 15 larger than clean Cu(111)! The open circle at $\theta_{Cs} = 0$ shows the rate obtained when the same dosing and reaction procedure used for Cs-dosed surfaces was repeated, except here pure water (without CsOH) was used. The rate is nearly the same as for clean Cu(111), which proves that the rate increase of fig. 2 is due to the Cs itself, rather than some impurity in the water droplet or some effect due to the water itself.

The concentrations of CsOH solution required to achieve the final coverages of fig. 2 were bigger than expected by a factor of at least 4. For

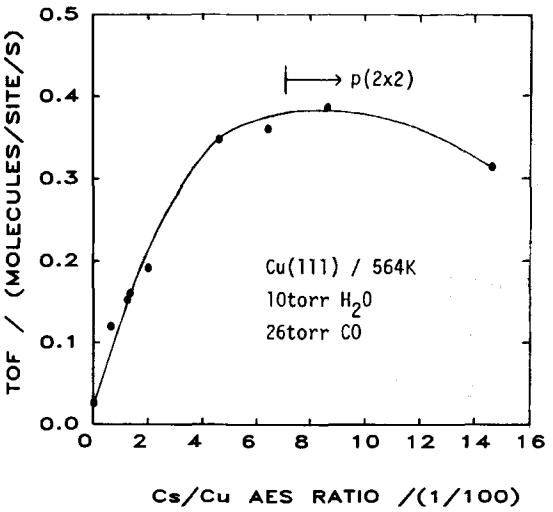

Fig. 3. Variation of the WGS rate with Cs coverage on Cu(111) at 564 K, 26 Torr CO and 10 Torr H_2O. The data here represent the average rate between 0.67 and 10.67 min reaction time.

Cs/Cu > 0.06, the required concentration increased more rapidly, so that, at the highest coverages, they were bigger by a factor of ~ 20. As will be shown below, this is largely due to a loss of Cs from the surface during the initial 40 s treatment in the reaction mixture, when the surface is reduced. We were unable to maintain Cs coverages higher than Cs/Cu ≃ 0.15 under reaction conditions, in spite of much larger initial Cs doses.

As shown in fig. 3, the reaction rate varies with θ_{Cs} in a very similar fashion at 564 K as was shown in fig. 2 at 612 K. Here we show the average rate over a reaction time period of ten minutes, after an initial treatment for 40 s at 612 K in a similar reaction mixture.

To establish if the rate-determining step or reaction mechanism changed on the Cs-promoted surface, we made a qualitative study of the reaction kinetics on the optimally-promoted surface (i.e., at a Cs/Cu AES ratio of 0.6–0.8). The reaction order with respect to H_2O partial pressure at 612 K and 26 Torr CO was about the same as on the clean surface (0.5–1.0). The apparent activation energy (20.5 ± 2.5 kcal mol^{-1}) at 10 Torr H_2O and 26 Torr CO increased slightly with respect to the clean surface (17.3 ± 1.8 kcal mol^{-1} [10]). (Here we use $\pm 2\sigma$ error bars.)

3.1.2. Cs surface structure

The surface structure of the Cs promoter in both the initial (as dosed) and final (after reaction) states was investigated in more detail using XPS, XAES and ISS at a Cs concentration which gave a final Cs/Cu AES ratio of 0.085.

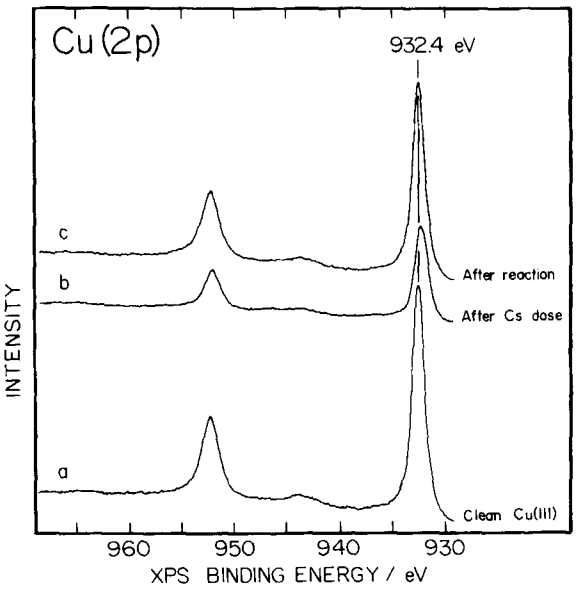

Fig. 4. Cu(2p) XPS spectra for: (a) clean Cu(111); (b) after dosing Cs with the procedure outlined in the text (final Cs/Cu AES ratio = 0.085); and (c) after treating surface (b) under reaction conditions (for five minutes at 612 K, 26 Torr CO and 10 Torr H_2O in figs. 4–9).

Fig. 4 shows the *Cu(2p) XPS* spectra for the clean surface, after dosing with the CsOH solution, and after treatment under reaction conditions (612 K, 26 Torr CO and 10 Torr H_2O) for five minutes. The freshly-dosed surface showed a Cu($2p_{3/2}$) peak which was strongly reduced in intensity and perhaps shifted to slightly ($\sim$ 0.15 eV) lower binding energy (BE) compared to clean Cu(111). When treated under reaction conditions, the peak returned to a very similar position and lineshape as the clean Cu(111) surface, with $\sim$ 82% of its original intensity.

The *Cu(LVV) XAES* spectra are shown in fig. 5. The freshly Cs-dosed surface showed a greatly reduced intensity, and a lineshape and position which were completely different from clean Cu(111). The main peak for the clean surface is at 335.1 eV BE (918.5 eV KE), and for the as-dosed surface it was at 337.1 eV BE (916.5 eV KE). These values are identical to those reported for bulk Cu and Cu_2O, respectively [17]. Except for some residual intensity from metallic Cu at 335.1 eV BE, the XAES lineshape for the as-dosed surface is also very similar to Cu_2O [17]. The Cu(2p) peak for the as-dosed surface (fig. 4) is also consistent with the reported spectrum of Cu_2O [17]. The difference spectrum of fig. 5 clearly shows that, upon treating upon reaction conditions, the Cu(LVV) spectrum returns to a shape characteristic of clean Cu(111), with only a slightly ($\sim$ 0%) reduced intensity due to the Cs overlayer.

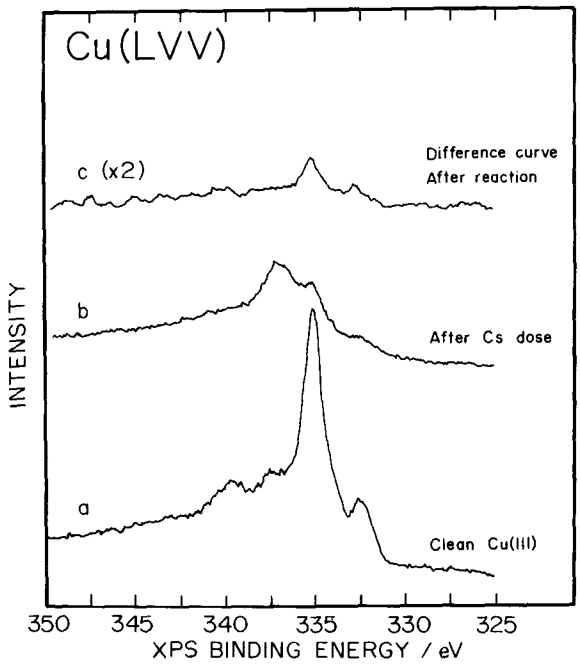

Fig. 5. Cu(LVV) XAES spectra for: (a) clean Cu(111); (b) the fresh Cs-dosed surface; and (c) the difference spectrum (X2) between clean Cu(111) minus the Cs-dosed surface after reaction. For (b) and (c), Cs/Cu = 0.085.

The *Cs(3d) XPS* spectra are shown in fig. 6. After extensive experiments with Cs, the nominally clean surface typically had a small residual $Cs(3d_{5/2})$ peak centered at 725.8 eV BE, as shown. This could only be removed by lengthy sputtering. The difficulty of its removal and its unusual energy suggest that it may be due to subsurface Cs. (Most bulk Cs^{1+} compounds have a $Cs(3d_{5/2})$ BE of ~ 723.5–724 eV [18].) The freshly-dosed surface showed a large $Cs(3d_{5/2})$ peak centered at 724.5 eV BE. This is close to the value for bulk CsOH (723.95 eV BE [18]). Upon treatment under reaction conditions, a large amount of Cs is lost from the surface region, as evidenced by the nearly four-fold decrease in Cs(3d) intensity. The peak also shifts to higher BE (725.1 eV).

The *O(1s) XPS* spectra are shown in fig 7. The as-dosed surface showed a large O(1s) peak centered at ~ 530.8 eV BE. This agrees with the values of 530.3 [18] and 530.8 eV BE [17] reported for bulk Cu_2O. The peak was also considerably broader than the instrumental resolution (FWHM = 2.3 eV), suggesting the presence of two non-equivalent oxygen atoms. A second peak at 531.9 eV BE was also noted for pure Cu_2O [17], which would be consistent

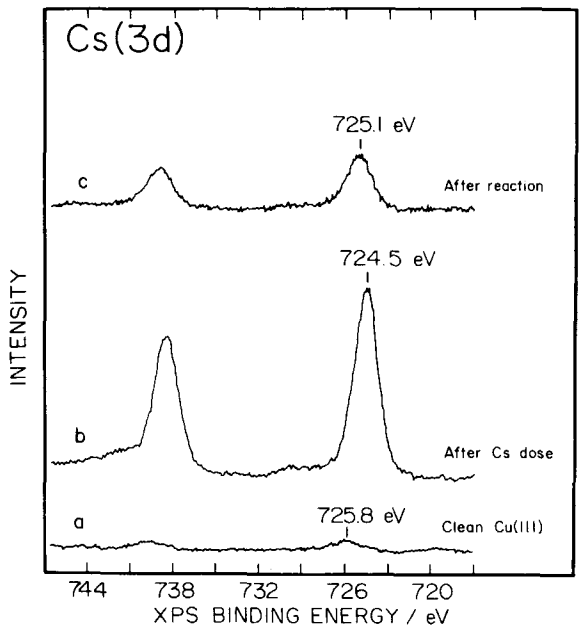

Fig. 6. Cs(3d) XPS spectra for: (a) nominally clean Cu(111); (b) the freshly Cs-dosed surface; and (c) surface (b) after treatment under reaction conditions. (Cs/Cu = 0.085.)

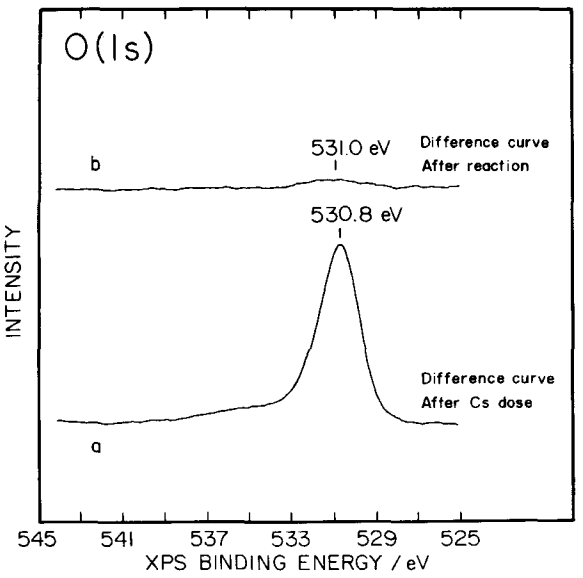

Fig. 7. O(1s) XPS spectra for: (a) freshly Cs-dosed Cu(111); and (b) after treating surface (a) under reaction conditions. (Cs/Cu = 0.085.)

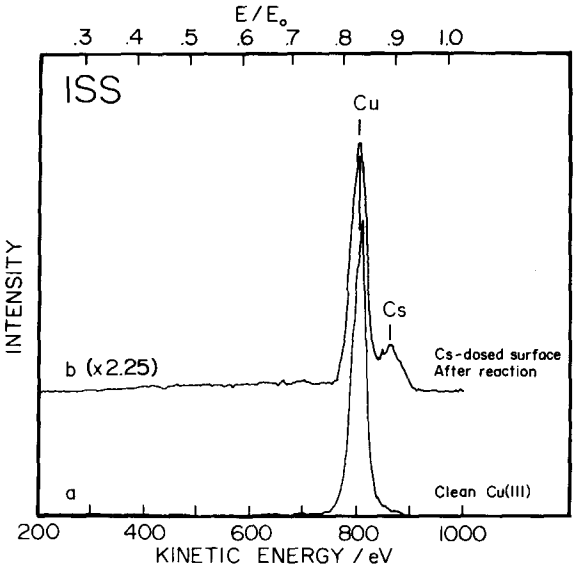

Fig. 8. He^+ ISS spectra for: (a) clean Cu(111); and (b) Cu(111) with Cs/Cu = 0.085, after treatment under reaction condition.

with this broadening. Bulk KOH shows an O(1s) peak at 531.5 eV BE [18], so that a species such as CsOH cannot be discounted. Following reaction, the O(1s) intensity decreased by a factor of at least 15. The peak is centered at ~ 531.0 eV BE, and is very broad (FWHM ≃ 2.8 eV).

Finally fig. 8 shows the He^+ ISS spectrum for the clean surface and for the Cs-dosed surface after treatment under reaction conditions (Cs/Cu = 0.085). One can see that the Cs/O overlayer attenuates the Cu ISS signal by a factor of ~ 2.5 to 40% of its clean value, and that a sizeable Cs peak appears. Note that the Cs mass peak appears some 20 eV lower in energy than expected based on simple kinematics [19]. Inelastic energy losses of this magnitude are not uncommon [20].

The spectra described above for the surface after treatment for five minutes in the reaction mixture was nearly the same as seen after only forty seconds reaction time. Thus, the observable surface structural changes occurring in the reaction mixture were essentially complete after only 40 s reaction time.

Information on the nature and stoichiometry of the Cs overlayers is also apparent in *electron-excited AES spectra.* As with XAES, the Cu(LVV) signal decreased and changed shape upon dosing Cs. As with the core-level XPS signals, the O(KVV) and Cs(MNN) signals and the O(KVV)/Cs(MNN) ratio for the as-dosed surface all decreased significantly upon brief treatment (~ 40 s) under reaction conditions. Thereafter, they decreased only very slowly. No

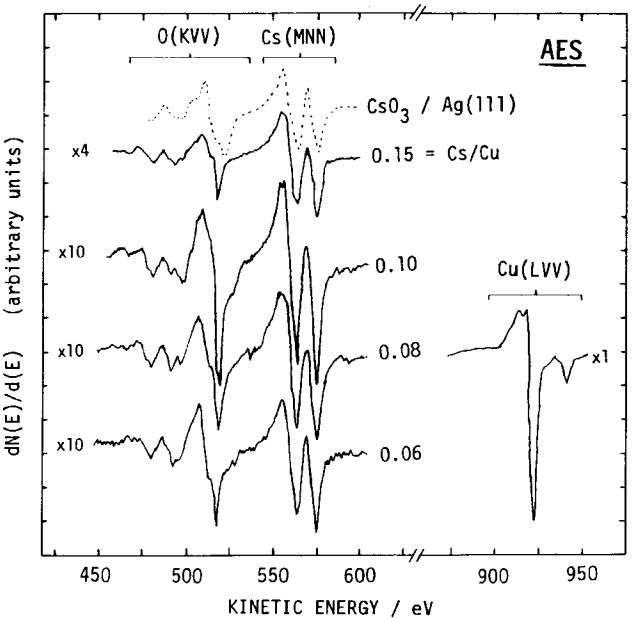

Fig. 9. Electron-excited AES spectra for the Cu(111) surface (solid curves) containing various Cs coverages, after treatment under reaction conditions. The dashed curve is for a Cs/O complex of ~1 : 3 stoichiometry on Ag(111), from ref. [21].

elements other than O, Cs, and Cu were seen in significant quantities. Example spectra for Cs-dosed surfaces after treatment as catalysts under reaction conditions are shown in fig. 9. One can see that the O(KVV)/Cs(MNN) AES ratio is roughly constant, independent of the Cs level. The constancy of this ratio suggests a Cs/O complex on the surface of fixed stoichiometry. (There may be hydrogen in this complex, since our analysis techniques are not sensitive to hydrogen.) For comparison, we show the AES spectrum for a Cs/oxygen complex on Ag(111) of Cs : O stoichiometric ratio ~1 : 3 [21]. One can see that the O(KVV) and Cs(MNN) AES lineshapes are completely different in the present case, with markedly narrower O(KVV) lines. Considering the effect of this narrowing on the integrated O(KVV) intensity, the Cs/O peak-to-peak height ratios then indicate a Cs : O stoichiometry of ~1 : 1.3 here.

The spectra shown in fig. 9 were recorded starting at 450 eV, immediately after the electron beam was turned on. This was done to minimize beam-damage effects. A second scan across the O/Cs region (on the same sample region) always showed a big (up to 40%) increase in the O(KVV) signal and a lineshape change, which we proved to be due to electron beam effects. The

O/Cs ratios were bigger for lower Cs coverages than those shown here, but we felt that this was due to the (relatively) increased contribution from this electron-induced oxygen buildup. The Cs/O overlayer for the surface after treatment under reaction conditions showed an attenuation of the Cu(LVV) AES intensity relative to clean Cu(111). Typical signal decreases were 11% for Cs/Cu = 0.082, and 23% for Cs/Cu = 0.146.

We should point out that the Cs/Cu ratio continued to decrease very slowly during reaction at 612 K, even after a few minutes reaction time. We attribute this to slow loss of Cs, via desorption or diffusion of Cs into the bulk of the Cu crystal. The rate of this process increased rapidly with Cs coverage, and was significant only for Cs/Cu ratios above ~ 0.05.

As indicated in figs. 2 and 3, the surface displayed a sharp p(2 × 2) LEED pattern after reaction (for > 2 min reaction time) at both 612 and 564 K, provided the Cs/Cu AES ratio exceeded ~ 0.067. Note that the first appearance of the p(2 × 2) pattern also coincides with the maximum in the reaction rate versus Cs coverage. The p(2 × 2) pattern was still apparent after reaction for the highest achievable Cs coverages. Interestingly, pure, metallic Cs on Cu(111) also shows a p(2 × 2) close-packed monolayer at $\theta_{Cs} = 0.25$ [22]. We feel that this cannot be the same structure, since desorption of a pure Cs monolayer generally begins at about 320 K on transition metals [21]. Our p(2 × 2) structure was stable to heating in UHV to above ~ 550 K. (The surface had to be cooled for LEED observation.) Interestingly, when oxygen is added to a pure p(2 × 2)-Cs monolayer on Cu(111), a p(2 × 2) pattern is again seen at an oxygen exposure which gives a minimum in the work function [22].

3.1.3. Cs coverage calibration

Several factors must be considered in assigning an absolute coverage scale to the Cs/Cu AES ratio discussed here. In this calibration, we assign the highest coverage obtainable after reaction (Cs/Cu ≃ 0.15) to $\theta_{Cs} = 0.25$. This is consistent with the observed p(2 × 2) LEED pattern, where there is one Cs atom per p(2 × 2) unit cell. It implies that the Cs/O complex starts nucleating into p(2 × 2) islands when θ_{Cs} exceeds 0.12. The attenuation of the Cu AES and XPS signals is also consistent with this coverage assignment. A close-packed monolayer of Cs atoms on Cu(111) ($\theta_{Cs} = 0.25$ [22]) should have a thickness of ~ 5.2 Å (assuming the bulk Cs density). Since metal oxides often have close to the same density as the bulk metal (in metal atoms per cm^3), we can assume that our complete p(2 × 2) Cs/O overlayer has approximately this same thickness (~ 5.2 Å). The 23% attenuation of the Cu(920 eV) AES peak at $\theta_{Cs} = 0.25$ then implies an electron inelastic mean-free-path (IMFP) of ~ 20 Å. This value fits well the tabulated IMFPs of Seah and Dench [23]. Similarly, the 18% attenuation of th Cu(2p) peak for Cs/Cu = 0.085 (or $\theta_{Cs} = 0.14$) suggests an IMFP of ~ 14 Å for these 321 eV photoelectrons, which is well within the range reported by Seah and Dench [23].

Let us now discuss the O/Cu and O/Cs AES ratios. From a study of atomically-adsorbed oxygen on this surface [10], we know that an O/Cu AES ratio of 0.15 corresponds to a coverage $\theta_O = 0.45$. The spectra of fig. 9 gave O/Cu ratios of 0.055 to 0.083, which then suggests oxygen coverages (θ_O) between 0.16 and 0.25. As we said above, by comparison to the AES spectra for an overlayer of stoichiometry of about CsO_3 on Ag(111), the spectra of fig. 9 indicate a stoichiometry here of about $CsO_{1.3}$. Combining this ratio with the oxygen coverages above suggests Cs coverages (θ_{Cs}) in fig. 9 between 0.12 and 0.19. These values are relatively consistent with the values based upon our coverage calibration of the Cs/Cu ratio, which gives θ_{Cs} between 0.10 and 0.25 in fig. 9.

Finally, for Cs overlayers on Ag(111), a Cs/Ag AES ratio of 0.033–0.050 is obtained at $\theta_{Cs} = 0.25$ [21]. The reported bulk AES sensitivity ratio of Ag : Cu is ~ 4.3 [24]. We thus expect a Cs/Cu AES ratio approximately in the range 0.14–0.22 at $\theta_{Cs} = 0.25$, which is consistent with our present calibration (0.15).

In general, we can say that the above intensity and attenuation comparisions in XPS and AES rule out the possibility that the p(2 × 2) LEED structure is really three domains of a p(2 × 1), since this would require coverages twice as large as those assigned above.

3.2. *Sulfur poisoning of Cs-promoted Cu(111)*

As noted in the introduction, the major limitation of Cu/ZnO catalysts for the water–gas shift reaction is not their inherent activity, which is relatively good, but their sensitivity to sulfur poisoning. Thus, the promotion in activity brought about by cesium addition would be especially important if it somehow also lead to a more sulfur-tolerant catalyst. To investigate this point, we have studied the interaction of H_2S with the Cs-promoted Cu(111) surface, and the resultant poisoning of the water–gas shift reaction.

At 300 K and above, H_2S dissociatively adsorbs on clean Cu(111) to liberate H_2 gas, depositing sulfur adatoms [11]. The sticking probability at 300 K is ~ 0.057, and almost constant with coverage until the surface is nearly saturated at $\theta_{Cs} \simeq 0.39$ [11]. We measured a sulfur uptake curve at 300 K for the Cs-promoted Cu(111) surface ($\theta_{Cs} = 0.15$) which was very similar to that reported for clean Cu(111) [11]. (For this experiment, the Cs-dosed surface was first reduced in the reaction mixture to achieve its final form characteristic of water–gas shift conditions.) The result indicates that the rate of sulfur deposition of the Cu catalyst is essentially the same with or without Cs addition, and that the saturation sulfur coverage is only slightly (~ 15%) smaller. In addition, the nature of the resulting sulfur adlayer is not greatly different in the presence or absence of Cs, as was evidenced by the essentially invariant S(2p) XPS peak position (162.5–162.6 eV BE). In addition, the Cu ISS signal was masked by sulfur addition in a manner similar to the clean

surface [11], while the Cs signal was not strongly influenced by sulfur addition. This suggests that, as on clean Cu(111) [11], the sulfur adatoms are bonded *above* Cu sites on the surface, and that the Cs either sits between or above the sulfur adatoms.

The WGS reaction rate on the Cs-promoted Cu(111) surface decreased with sulfur coverage in a fashion similar to that seen on clean Cu(111) [11], provided the curves are normalized to the sulfur-free rate in each case. On the clean surface. This poisoning was interpreted in terms of simple site-blocking by the sulfur adatoms [11]. Since the rate on the Cs-dosed surface starts out so much higher in the absence of sulfur, these results indicate that the Cs-promoted surface can tolerate considerably higher sulfur content in the reactant feed while maintaining the activity of the unpromoted catalyst.

4. Discussion

The XPS/XAES data indicate that the Cs dosing procedure used here results in a surface with a Cu_2O film of > 20 Å thickness, and a Cs overlayer with Cs^{1+} character. Upon treatment for ≥ 40 s under WGS reaction conditions, the Cu is completely reduced to a metallic Cu(111) surface, and some Cs is lost from the surface region. The remaining $Cs(3d_{5/2})$ peak shifts to slightly higher BE (by ~ 0.6 eV) during this reduction process. In a similar study of potassium overlayers deposited on Fe from aqueous KOH solution, the K(2p) peak also increases in BE (~ 0.3 eV) upon reduction [25]. Furthermore, vapor-deposited potassium on Pt(111) and Fe(110) show a K(2p) peak which decreases by 0.5–1.0 eV in BE upon oxidation [26–27]. These shifts are difficult to interpret, and cannot be easily related to changes in the oxidation state of the alkali. Differences in final-state relaxation energy may be dominating here. A decrease in core-level binding energy upon the bulk oxidation of Ba has been explained in terms of initial-state differences, where a strong decrease in the spatial extent of occupied valence orbitals accompanies oxidation [28].

In any case, the roughly constant Cs/O AES ratio seen here indicates an oxidic or hydroxidic Cs surface compound on the reduced surface. The Cs : O stoichiometry in this overlayer is $\sim 1:1.3$. At $\theta_{Cs} > 0.12$, this overlayer nucleates into $p(2 \times 2)$ islands, which we assign to a local coverage $\theta_{Cs} = 0.25$ within the islands.

The surface Cs here is thermodynamically stabilized by the presence of oxygen (or hydroxide) in the surface complex. The broad O(1s) peak at ~ 531 eV BE for the reduced Cs overlayer can be compared to assignments of 530, 531.5, and 533.3 eV for O_1, OH_a, and H_2O_a, respectively, on Cu(111) [29], or 529.5–530.1, 530.8, and 533.4 eV for these species on Cu(110) [30]. This comparison favors a hydroxide assignment, although the presence of Cs here

makes such a comparison tenuous. On K-dosed Pt(111), water adsorption leads to an alkali–OH complex of stoichiometry K : O = 1 : 1.3 with an O(1s) peak at 531 eV BE [14], similar to our post-reaction complex. On Pt(111), this complex is stable to 570 K in vacuum [14]. Our complex was stable to above 550 K in vacuum. Similarly, a KOH species is formed on Ru(001) by the interaction of H_2O with adsorbed potassium [12], which decomposes between 500 and 600 K via KOH → K + O + H. Pure Cs on Cu(111) should desorb at a much lower temperature, as noted above.

The ISS method used here is sensitive only to the topmost atomic layer of the solid [20]. The attenuation of the Cu signal and the clear appearance of a Cs signal for the reduced overlayer at $\theta_{Cs} = 0.14$ proves that the Cs forms an overlayer *above* the topmost Cu(111) plane. The magnitude of the attenuation of the Cu signal (60% down from clean Cu) is consistent with the fact that the Cs coverage was ~ 57% of its saturation level.

The slow decay in WGS rate with reaction time (above 40 s) shown in fig. 1 was not accompanied by large changes in the surface structure, which mostly occurred in the initial 40 s reaction time. The only changes that occurred after 40 s were a slow loss in Cs (and oxygen) AES or XPS signal and a strengthening of the p(2 × 2) LEED pattern. The decrease in WGS rate could not be directly attributed to the loss of Cs, since the coverage remained in a range (0.12–0.15) near the flat maximum of fig. 2. On the other hand, the ordering of the overlayer could have a large influence. Notice in figs. 2 and 3 that the rate increases with θ_{Cs} until the p(2 × 2) LEED pattern starts to nucleate. With further increases in θ_{Cs}, the rate remains constant or even decreases. This indicates that the p(2 × 2) structure may not be as active as the disordered structures at slightly lower local coverage. The rate decrease with reaction time could then be related to growth of p(2 × 2) domain size.

The WGS kinetics on clean Cu(111) have been interpreted [10] in terms of a mechanism whereby the rate-determining step is the dissociative adsorption of H_2O, at least under the reaction conditions used in this paper. The coverage of adsorbed H_2O under reaction conditions should be low [10], which is consistent with the strong dependence in the rate upon H_2O pressure [10]. That dependence is the same for the Cs-promoted surface, which suggests that a similar situation pertains here for Cs-dosed Cu(111).

According to that model used on clean Cu(111) [10], the apparent activation energy for WGS (E_{app}) is really the difference between the activation energy for the dissociation of adsorbed H_2O (E_{diss}) and the desorption energy for H_2O (E_{des}): $E_{app} = E_{diss} - E_{des}$. Since E_{app} increases from 17 to ~ 20 kcal mol^{-1} upon Cs promotion, this relationship indicates that E_{diss} increases upon Cs addition, and/or E_{des} decreases. We would not expect Cs to cause E_{des} to drop compared to ~ 10 kcal mol^{-1} on clean Cu(111) ([10] and references therein), since alkali addition generally slightly increases the adsorption energy for H_2O on transition metals [12–14,33,36]. Therefore, the activation energy

for the dissociation of adsorbed water must increase from ~ 27 to at least 30 kcal mol^{-1} upon Cs addition. The 15-fold increase in the WGS rate is therefore (within this model) *not* related to reducing the energy barrier for the reaction. Instead, it must be due to an increase in the pre-exponential factor for the dissociation of adsorbed H_2O (ν_{diss}). On clean Cu(111), ν_{diss} was estimated to be $\sim 8 \times 10^{11}$ s^{-1} [10]. To compensate for both the increased rate and the increased activation energy, the corresponding value for the Cs-dosed surface must be at least 170-fold bigger, or $\sim 1 \times 10^{14}$ s^{-1}. The increased WGS activity is therefore due to a large increase in the frequency factor for the dissociation of adsorbed H_2O.

Alkali additives are known to have strong electronic influences upon transition metal surfaces, which can lead to relatively long-range changes in their chemisorption behavior ([34] and references therein). While such influences upon the Cu are certainly expected with Cs addition, one generally thinks of these as subtly modifying the potential energy surface for the adsorbate/surface interaction, rather than drastically altering the frequency factor for some step in that interaction. Thus, a change in activation energy with a relatively constant frequency factor is symptomatic of such *indirect* influences of an additive upon some adsorption step. The 170-fold increase in ν_{diss} suggested here is indicative instead of *direct* participation of Cs in the rate-limiting step. For this reason, we tentatively propose a mechanism for Cs promotion whereby water dissociation occurs at the surface Cs complex. One example pathway is shown in scheme 1. Two hydrogen adatoms then associatively desorb to produce H_2. In the proposed formate mechanism [1,3,6,8,10], the OH_a formed above reacts with CO to make the formate intermediate ($HCOO_a$), which then decomposes into $CO_2 + H_a$. In the alternate surface redox mechanism [1,4,10], the OH_a dissociates further to $O_a + H_a$. The O_a then reacts with CO to make CO_2.

On clean Cu(111), extrapolation of CO desorption kinetics indicated that the CO coverage under our reaction conditions should be quite small [10]. Nevertheless, the WGS reaction rate was independent of CO pressure. This meant that the rate was also independent of CO coverage. This was interpreted to indicate that the consumption of water fragments via further reaction with CO_a was very rapid compared to the rate at which these fragments are deposited on the surface (via H_2O dissociation) [10]. We expect that the addition of the Cs surface complex will increase the adsorption energy for CO

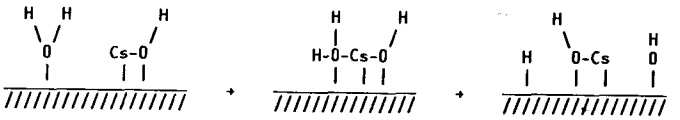

Scheme 1.

on Cu(111) (as is usually the case for alkali addition to transition metals [34,35]). This effect would lead to an increase in the steady-state CO coverage under reaction conditions, compared to the unpromoted surface. Since the WGS rate is independent of CO coverage even without Cs, we do not expect this to substantially affect the kinetics or the kinetic analyses outlined above. However, it may be that the presence of the Cs complex increases the adsorption energy for CO by such a great extent that the CO coverage under reaction conditions actually now approaches saturation. If this were the case, we would expect to see a *negative* reaction order with respect to CO pressure, since CO_a would now inhibit the dissociative adsorption of H_2O. (Unfortunately, we neglected to measure the CO reaction order on the Cs-promoted surface.) If indeed this turns out to be the case, a much more complicated kinetic analysis will be required than the simple low-coverage limit used above.

In any case, the rate constant for the dissociation of H_2O_a increases by *at least* a factor of 15 upon Cs promotion (and even more if CO_a substantially inhibits water adsorption via site blocking). This result should perhaps not be too surprising, since alkali addition enables the dissociation of H_2O_a at temperatures as low as 100 K on Pt(111) [14] and Ru(001) [12,13]. However, no water dissociation was noted in coadsorption with Na on Cu(110) [33]. Furthermore, adsorbed water desorbs molecularly, with no noticeable dissociation, from Cs-dosed Ag(110) [36]. Clearly, a better knowledge of the influences of Cs and of this surface Cs/O compound upon the adsorption/desorption behavior of H_2O and of CO on Cu(111) is needed before a more definitive picture of the promotion mechanism evolves.

Klier and coworkers [7,8] have recently reported that Cs addition causes a 2.0–2.5-fold increase in the rate of WGS on high-surface-area Cu/ZnO catalysts. In that case, the reaction temperature was considerably lower (510–525 K), and the reaction rate was measured under methanol-synthesis conditions near 75 atm pressure. To compare our present 15-fold increase to their results, we must correct for the temperature difference and the difference in apparent activation energies for clean versus Cs-doped Cu (-3 kcal mol^{-1}). Thus, our 15-fold increase at 612 K reduces to a 9-fold increase at 510 K. This is still considerably larger than the observed effect on Cu/ZnO. The difference may be related to the fact that, under their higher-pressure conditions, the dissociative adsorption of H_2O does not completely determine the reaction rate. Klier and coworkers [8] mention a similar role for Cs, except in their mechanism the hydroxyl group remains associated with the Cs until it attacks CO to make the formate intermediate: $Cs^+OH^- + CO \rightarrow HCOO^-Cs^+$. Direct participation in the reaction by the oxygen atoms of the surface Cs/O complex should be tested by isotopic tracing.

Acknowledgements

One of us (C.T.C.) would like to acknowledge partial support of this work by the US Department of Energy, through Morgantown Energy Technology Center. Another (B.E.K.) would like to acknowledge partial support of this work by the Department of Energy, Office of Basic Energy Sciences, Chemical Sciences Division. Helpful discussion with K. Klier and J. Hrbek are appreciated. Help with data manipulation by M.T. Paffett is also appreciated, as is typing by B. McGaw.

References

[1] D.S. Newsome, Catalysis Rev.-Sci. Eng. 21 (1980) 275.
[2] F. Garbassi and G. Petrini, J. Catalysis 90 (1984) 106, 113.
[3] T. van Herwijnen and W.A. de Jong, J. Catalysis 63 (1980) 83, 94.
[4] E. Fiolitakis and H. Hofmann, J. Catalysis 80 (1983) 328.
[5] T.M. Yurieva and T.P. Minyukova, Reaction Kinet. Catalysis Letters 29 (1985) 55.
[6] D.C. Grenoble, M.M. Estadt and D.F. Ollis, J. Catalysis 67 (1981) 90.
[7] K. Klier, C.W. Young and J.G. Nunan, Ind. Eng. Chem. Fundamentals 25 (1986) 36.
[8] D.C. Bybell, P.P. Deutsch, R.G. Herman, P.B. Himmelfarb, J.G. Nunan, C.W. Young, C.E. Bogdan, G.W. Simmons and K. Klier, Preprints Petroleum Div. Am. Chem. Soc. 31 (1986) 282.
[9] G. Vlaic, J. Bart, W. Cavigiolo, B. Pianzola and S. Mobilio, J. Catalysis 96 (1985) 314.
[10] C.T. Campbell and K.A. Daube, J. Catalysis 104 (1987) 109.
[11] C.T. Campbell and B.E. Koel, Surface Sci. 183 (1987) 100.
[12] P.A. Thiel, J. Hrbek, R.A. DePaola and F.M. Hoffmann, Chem. Phys. Letters 108 (1984) 25.
[13] D.L. Doering, S. Semancik and T.E. Madey, Surface Sci. 133 (1983) 49.
[14] M. Kiskinova, G. Pirug and H.P. Bonzel, Surface Sci. 150 (1985) 319.
[15] C.T. Campbell and K.A. Daube, J. Catalysis, in press.
[16] J.R. Moody and R.M. Lindstrom, Anal. Chem. 49 (1977) 2264.
[17] B.R. Strohmeier, D.E. Leyden, R.S. Field and D.M. Hercules, J. Catalysis 94 (1985) 514.
[18] C.D. Wagner, W.M. Riggs, L.E. Davis, J.F. Moulder and G.E. Muidenberg, Handbook of X-ray Photoelectron Spectroscopy (Perkin-Elmer, Eden Prairie, MN, 1979).
[19] H. Niehus and E. Bauer, Surface Sci. 47 (1975) 222.
[20] H. Niehus and G. Comsa, Nucl. Instr. Methods. B13 (1986) 213.
[21] C.T. Campbell, J. Phys. Chem. 89 (1985) 5789.
[22] S.A. Lindgren and L. Walldén, Surface Sci. 80 (1979) 620; Phys. Rev. B22 (1980) 5967.
[23] M.P. Seah and W.A. Dench, Surface Interface Anal. 1 (1979) 2.
[24] L.E. Davis, N.C. MacDonald, P.W. Palmberg, G.E. Riach and R.E. Weber, Handbook of Auger Electron Spectroscopy (Perkin-Elmer, Eden Prairie, MN, 1976).
[25] H.P. Bonzel, G. Broden and H.J. Krebs, Appl. Surface Sci. 16 (1983) 373.
[26] G. Pirug, H.P. Bonzel and G. Broden, Surface Sci. 122 (1981) 1.
[27] G. Pirug, G. Broden and H.P. Bonzel, Surface Sci. 94 (1980) 323.
[28] G.K. Wertheim, J. Electron Spectrosc. Related Phenomena 34 (1984) 309.
[29] C.T. Au, J. Breza and M.W. Roberts, Chem. Phys. Letters 66 (1979) 340. (See also ref. [31].)
[30] A. Spitzer and H. Luth, Surface Sci. 160 (1985) 353. (See also ref. [31].)
[31] Beam damage or impurities may have been the source of water dissociation on Cu in refs. [29,30], as pointed out in ref. [32].

[32] J.K. Sass and N.V. Richardson, Surface Sci. 139 (1984) L204.
[33] K. Bange, D. Grider and J.K. Sass, Surface Sci. 126 (1983) 437.
[34] K. Uram, N. Lily, M. Folman and J.T. Yates, Jr., J. Chem. Phys. 84 (1986) 2891.
[35] D. Lackey, M. Surman, S. Jacobs, D. Grider and D.A. King, Surface Sci. 152/153 (1985) 513.
[36] E.M. Stuve, R. Dohl-Oelze, K. Bange and J.K. Sass, J. Vacuum Sci. Technol. A4 (1986) 1307.